

# UC Berkeley

## UC Berkeley Previously Published Works

### Title

Effect of Ligand Structure on the Electron Density and Activity of Iridium Catalysts for the Borylation of Alkanes

### Permalink

<https://escholarship.org/uc/item/0x39651m>

### Journal

ACS Catalysis, 10(5)

### ISSN

2155-5435

### Authors

Larsen, Matthew A  
Oeschger, Raphael J  
Hartwig, John F

### Publication Date

2020-03-06

### DOI

10.1021/acscatal.0c00152

Peer reviewed



# HHS Public Access

Author manuscript

*ACS Catal.* Author manuscript; available in PMC 2020 November 10.

Published in final edited form as:

*ACS Catal.* 2020 March 6; 10(5): 3415–3424. doi:10.1021/acscatal.0c00152.

## Effect of Ligand Structure on the Electron Density and Activity of Iridium Catalysts for the Borylation of Alkanes

**Matthew A. Larsen,**

Department of Chemistry, University of California, Berkeley, California 94720, United States;

**Raphael J. Oeschger,**

Department of Chemistry, University of California, Berkeley, California 94720, United States

**John F. Hartwig**

Department of Chemistry, University of California, Berkeley, California 94720, United States;

### Abstract

An in-depth study of iridium catalysts for the borylation of alkyl C–H bonds is reported. Although the borylation of aryl C–H bonds can be catalyzed by iridium complexes containing phen or bpy ligands at mild temperatures and with limiting arene, the borylation of alkyl C–H bonds remains underdeveloped. We prepared a library of phenanthrolines that contain varying substitution patterns. The corresponding phen–Ir trisboryl carbon monoxide complexes were synthesized to determine the electron-donating ability of these ligands, and the initial rates for the borylation of the C–H bonds in THF and diethoxyethane  $\beta$  to oxygen catalyzed by Ir complexes containing these ligands were measured. For some subsets of these ligands, the donor ability correlated positively with the rate of C–H borylation catalyzed by the complexes containing ligands within a given subset. However, across subsets, ligands possessing similar donor properties to one another form catalysts for the borylation of alkyl C–H bonds with widely varying activity. This phenomenon was investigated computationally, and it was discovered that the stabilizing interactions between the phenanthroline ligand and the boryl ligands attached to Ir in the transition state for C–H oxidative addition could account for the differences in the activity of the catalysts that possess similar electron densities at Ir. The effect of these interactions on the borylation of secondary alkyl C–H bonds is larger than it is on the borylation of primary alkyl C–H bonds.

### Graphical Abstract

---

**Corresponding Author: John F. Hartwig** – Department of Chemistry, University of California, Berkeley, California 94720, United States; jhartwig@berkeley.edu.

Author Contributions

The manuscript was written through contributions of all authors. All authors have given approval to the final version of the manuscript.

Supporting Information

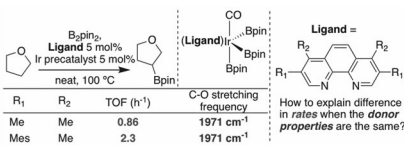
The Supporting Information is available free of charge at <https://pubs.acs.org/doi/10.1021/acscatal.0c00152>.

Experimental procedures and spectra for all new compounds, Cartesian coordinates and energies of calculated ground states and transition states, and crystallographic information (PDF)

CIF files (CIF)

Complete contact information is available at: <https://pubs.acs.org/10.1021/acscatal.0c00152>

The authors declare no competing financial interest.



## Keywords

C–H borylation; catalyst design; reaction kinetics; iridium; phenanthrolines; alkane functionalization

## INTRODUCTION

The functionalization of C–H bonds is a powerful and direct strategy in organic synthesis to diversify molecules and to reduce the number of steps in a synthetic sequence.<sup>1–3</sup> Over the last two decades, many catalytic methods have been developed that follow this strategy, and these methods include those in which the C–H bond cleavage is guided by a directing group contained within the substrate and those in which the C–H bond cleavage is undirected.<sup>4</sup> Undirected C–H bond functionalizations are more difficult to achieve than directed functionalizations, and the borylation of C–H bonds is arguably among the most useful. The C–B bond of the organoboronate esters formed from this reaction can be transformed to a variety of C–C and C–heteroatom bonds. Furthermore, the selectivity of C–H borylation is often orthogonal to that of other C–H bond functionalizations.<sup>5</sup> However, while the undirected borylation of aryl C–H bonds is a versatile, practical method now used on a relatively large scale in industry,<sup>6</sup> the undirected borylation of alkyl C–H bonds remains underdeveloped.

First reported in 2002 by Ishiyama, Miyaura, and Hartwig, the reaction of an arene with B<sub>2</sub>pin<sub>2</sub> (bispinacolatodiboron) catalyzed by the combination of [Ir(COD)OMe]<sub>2</sub> and 4,4'-*tert*-butylbipyridine (dtbpy) forms arylboronate esters in high yield at room temperature and without the need for excess arene (Scheme 1a).<sup>7,8</sup> In stark contrast, the borylation of alkyl C–H bonds catalyzed by Rh,<sup>9</sup> Ru,<sup>10</sup> or Ir<sup>11,12</sup> catalysts requires high temperatures and, with few exceptions,<sup>13,14</sup> a large excess of the alkane (Scheme 1b). While strategies for the borylation of alkyl C–H bonds involving directing groups have been developed that overcome these limitations,<sup>15–19</sup> the requirement that a specific functional group be contained in the substrate limits the generality of these methods. Thus, novel catalysts with high activity for the undirected borylation of alkyl C–H bonds could create new capabilities in organic synthesis.

In 2012, our group reported an Ir catalyst for the borylation of alkyl C–H bonds,<sup>11</sup> including the secondary alkyl C–H bonds of amines and ethers.<sup>20</sup> We found that the combination of an Ir precursor and 3,4,7,8-tetramethylphenanthroline (tmphen) catalyzes the borylation of neat alkanes with B<sub>2</sub>pin<sub>2</sub> at 100–120 °C, temperatures that are lower than those reported for the borylation of alkanes catalyzed by Rh or Ru catalysts. Since this initial report, there have been several examples of the C–H borylation of arenes and alkanes catalyzed by Ir bound to various phenanthrolines.<sup>14,21–23</sup> Given this broad utility of Ir–phenanthroline catalysts for C–H borylation and the potential diversity of phenanthroline derivatives that could be

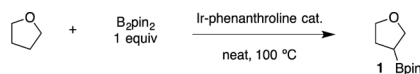
synthesized, we initiated a study to examine the effect of the substituents on the phenanthroline ligands for various properties of phenanthroline-bound Ir catalysts, with the goal of identifying structural features that can lead to highly active catalysts for the C–H borylation of alkanes.

Here, we report a detailed study of the effect of the structure of phenanthroline ligands on the rates of alkyl C–H borylation catalyzed by the corresponding Ir–phenanthroline catalysts. We measured the rates of the reactions catalyzed by complexes containing a series of ligands and prepared the corresponding phenanthroline-ligated iridium trisboryl complexes bound by carbon monoxide. The C–O stretching frequency of these complexes was correlated with the natural log of the rate constant for alkyl C–H borylation to ascertain the effect of the electron density at the metal center on the rates of alkyl C–H borylation. Lastly, we report computational and experimental studies that support the existence of weak interactions in the transition state for turnover-limiting oxidative addition of alkyl C–H bonds. These weak interactions have a large impact on the rate of the turnover-limiting oxidative addition step.

## RESULTS AND DISCUSSION

### Ligand Design and Synthesis.

To reveal the effect of the electronic properties of phenanthroline-bound Ir catalysts on the rate of the borylation of an alkyl C–H bond, we studied the C–H borylation of THF as a model reaction. The borylation of tetrahydrofuran to form 3-boryl-tetrahydrofuran **1** (eq 1) was chosen over the borylation of simple



(1)

hydrocarbons as the model reaction because of the poor solubility of phenanthrolines in alkanes. Furthermore, the yield of the borylation of THF catalyzed by Ir–phenanthroline complexes is higher than that of the borylation of hydrocarbons catalyzed by similar complexes.<sup>11,12</sup>

A series of phenanthrolines containing various substituents that would vary the electronic properties of the ligand were synthesized, and the rates of the borylation of THF catalyzed by complexes of these phenanthrolines were measured. The phenanthroline core has six positions that can bear substituents (Figure 1a). Substituents at the 5 and 6 positions of the backbone of the phenanthroline are synthetically difficult to vary. However, substituents at the 3 and 8 positions ( $\beta$  to nitrogen) and the 4 and 7 positions ( $\gamma$  to nitrogen) can be varied easily and without changing the steric environment near the metal center. Thus, we synthesized a library of symmetrical phenanthrolines that contain various substituents at positions 3, 4, 7, and 8.

The effect of substituents at the 4 and 7 positions of phenanthrolines bound to Ir on the electron density at Ir is likely to be larger than that of substituents at the 3 and 8 positions due to  $\pi$  donation and  $\pi$  acceptance to and from the metal center. Thus, we synthesized phenanthrolines containing a variety of substituents at the 4 and 7 positions.

Although the effect of the 3,8 substituents of phenanthrolines on the electron-donating ability of these ligands is likely less significant than that of the 4,7 substituents, most reported Ir-phenanthroline catalysts for C-H borylation contain substituents at the 3 and 8 positions, such as methyl<sup>11</sup> or mesityl,<sup>18</sup> suggesting that these substituents have an influence on the activity or stability of the corresponding catalysts. Thus, we synthesized three groups of phenanthrolines: one containing no substituents at the 3 and 8 positions, one containing methyl substituents at the 3 and 8 positions, and one containing mesityl substituents at the 3 and 8 positions (Figure 1b). Each of these groups comprised phenanthrolines containing various 4,7 substituents including chloro, hydro, methyl, silylmethyl, and pyrrolidinyl.

The group of phenanthrolines lacking 3 and 8 substituents is shown in Scheme 2. This group contains some previously reported phenanthrolines and some novel phenanthrolines. Dichlorophenanthroline **2a** was synthesized according to a known method,<sup>24</sup> and phenanthrolines **2b** and **2c** were purchased from commercial sources. The disilylmethylphenanthroline **2d** was synthesized from **2c** by deprotonation of the 4,7-dimethyl motif, followed by quenching with triisopropylsilyl triflate (TIPSOTf). Lastly, **2e** was synthesized from **2a** by nucleophilic aromatic substitution with pyrrolidine.

Phenanthrolines for the current study containing the 3,8-dimethyl motif are shown in Scheme 3. The synthesis of **3a** was conducted according to a known procedure.<sup>25</sup> Dimethylphenanthroline **3b** is typically synthesized by a Skraup reaction,<sup>26</sup> but the yield is very low, and separation of **3b** from the reaction mixture is difficult. We considered the conversion of 3,8-dibromophenanthroline to **3b** by Pd-catalyzed Negishi coupling. With dimethylzinc as the nucleophile, **3b** was formed in low yield, but with TMSCH<sub>2</sub>ZnCl as the nucleophile, **3b** formed in good yield following treatment of the crude mixture with methanolic KOH. Tetramethylphenanthroline **3c** was purchased from a commercial source. The synthesis of 3,8-dimethyl-4,7-disilylmethyl-phenanthroline **3d** from **3c** was conducted in analogy to the synthesis of **2d**. The synthesis of 3,8-dimethyl-4,7-dipyrrolidinylphenanthroline **3e** from **3a** was conducted in analogy to the synthesis of **2e**.

To synthesize the group of phenanthrolines containing the 3,8-dimesityl motif (Scheme 4), we developed an approach involving site-selective cross-coupling. From dihydroxyphen,<sup>24</sup> 3,8-dibromo-4,7-dichlorophenanthroline was synthesized by bromination followed by deoxychlorination. The Negishi coupling of 3,8-dibromo-4,7-dichlorophenanthroline with MesZnCl formed **4a**, selectively. Phenanthroline **4b** was synthesized according to a known procedure.<sup>18</sup> Negishi coupling of **4a** with dimethylzinc afforded **4c** in good yield, and **4c** underwent silylation to form **4d** in analogy to the syntheses of **2d** and **3d**. Phenanthroline **4a** proved to be unreactive toward nucleophilic aromatic substitution with pyrrolidine, so a 4,7-dipyrrolidinyl analogue of 3,8-dimesityl phenanthroline was not synthesized.

## Synthesis of Phenanthroline-Bound Ir–Trisboryl Carbon Monoxide Complexes.

To gain information on how the structure of phenanthrolines affects the electronic properties of the intermediate of the catalytic process that cleaves the alkyl C–H bond, we synthesized a series of phenanthroline-bound Ir–trisboryl carbon monoxide complexes containing ligands **2–4**. By methods analogous to those we previously reported,<sup>27</sup> complexes **5a–e**, **6a–e**, and **7a–d** were synthesized. The C–O stretching frequencies of these complexes as a solution in THF were measured by infrared spectroscopy, and the values are shown in Table 1. Within each group of phenanthroline-ligated boryl complexes, the C–O stretching frequencies of the corresponding complexes decrease for various 4,7 substituents in the order Cl > H > Me > CH<sub>2</sub>TIPS > pyrrolidinyl. In other words, the electron density at Ir increases in the order Cl < H < Me < CH<sub>2</sub>TIPS < pyrrolidinyl. This ordering would be predicted based on the corresponding Hammett parameters of these substituents.<sup>28</sup>

Varying the 3 and 8 substituents to H, Me, or Mesityl had little effect on the electron density at Ir. However, based on the C–O stretching frequencies of complexes **5e** and **6e** (1963 and 1967 cm<sup>-1</sup>, respectively), pyrrolidinyl-substituted phen **2e** contained in complex **5e** is more donating than the analogous phen **3e** contained in complex **6e**. This difference in electron-donating ability is likely due to the steric hindrance of the methyl group ortho to the pyrrolidinyl group in **3e**; this group prevents the pyrrolidinyl group from adopting an ideal conformation for the nitrogen lone pair to donate into the pi system of the phen ligand.

For one of these complexes **6d**, crystals suitable for X-ray diffraction were obtained (Figure 2). This trisboryl–iridium carbon monoxide complex adopts a distorted octahedral geometry. The carbon monoxide ligand is tilted away from the phenanthroline ligand, as evidenced by the N1–Ir1–C1 and N2–Ir1–C1 angles of 106.51° and 100.79°, respectively. Furthermore, the carbon monoxide ligand is bent; the Ir1–C1–O1 angle is 171.60°. Perhaps surprisingly, the two bulky silylmethyl substituents of the phenanthroline contained in this complex are oriented toward the more hindered side of the complex. However, this conformation is likely a result of crystal-packing effects. The Ir–B distances (2.052 and 2.061 Å) of the two boryl ligands that are trans to the N atoms of the phenanthroline are similar to those for the boryl groups trans to the N atoms of a bipyridine ligand (2.027 and 2.057 Å) in the COE-bound dtbpy–Ir–trisboryl complex.<sup>7</sup> However, the Ir–B distance for the boryl ligand trans to CO (2.118 Å) in the structure of complex **6d** is significantly longer than that for the boryl ligand trans to COE (2.055 Å) in the structure of a COE-bound dtbpy–Ir–trisboryl complex.<sup>7</sup>

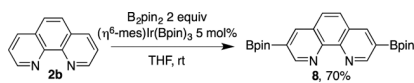
## Measurement of Rates of the Borylation of THF Catalyzed by Ir–Phenanthroline Complexes.

We conducted a series of reactions of THF with B<sub>2</sub>pin<sub>2</sub> at 100 °C catalyzed by the combination of the isolable trisboryl complex ( $\eta^6$ -mes)Ir(Bpin)<sub>3</sub><sup>29</sup> and each of the phenanthrolines **2–4** from our library of ligands. For specific reactions, this combination of ( $\eta^6$ -mes)Ir(Bpin)<sub>3</sub> and ligand will be referred to as Ir–**ligand** (e.g., Ir–**2a** for the combination of ( $\eta^6$ -mes)Ir(Bpin)<sub>3</sub> and phenanthroline **2a**). The combination of ( $\eta^6$ -mes)Ir(Bpin)<sub>3</sub> and the phenanthroline ligand forms the corresponding phenanthroline-bound iridium–trisboryl complex (the proposed active catalyst) in >90% yield (see the Supporting Information, pp. S33, for details). The initial rate of formation (<25% yield) of alkyl boronate **1** was

measured for each reaction by gas chromatography, and the final yield of **1** was measured after 48 h. Under the reaction conditions, no induction period was detected for the formation of **1**. From the initial rates of these reactions and the catalyst concentration, we determined the observed first-order rate constants ( $k_{\text{obs}}$ ) and correlated the log of these rate constants with the C–O stretching frequency of the corresponding trisboryl CO complexes **5–7**. These correlations are depicted graphically for phenanthrolines lacking 3 and 8 substituents (Figure 3a), phenanthrolines containing 3,8-dimethyl groups (Figure 3b), and phenanthrolines containing 3,8-dimesityl groups (Figure 3c). A superimposition of all three sets of correlations is provided in Figure 3d.

Because the oxidative addition of the C–H bond is presumed to be the turnover-limiting step of the C–H borylation of THF,<sup>11,20</sup> one might expect a positive correlation between the log of  $k_{\text{obs}}$  for this reaction catalyzed by Ir–(**2–4**) and the electron density at the metal center of Ir–(**2–4**) indicated by a negative correlation between  $\log(k_{\text{obs}})$  and the C–O stretching frequency of the corresponding complexes **5–7**. However, such a correlation was not observed for the borylation of THF catalyzed by Ir catalysts containing ligands **2a–e**, lacking 3 and 8 substituents (Figure 3a). For example, ligand **2e** is much more electron-donating than either ligands **2b** or **2c**, but the borylation of THF catalyzed by Ir–**2e** is slower than the borylation catalyzed by Ir–**2b** and Ir–**2c**.

One origin of this perturbation of the order of reactivity results from the modification of the ligand in the catalytic reaction. We discovered that the parent phenanthroline **2b** undergoes a rapid bisborylation at the 3 and 8 positions to form 3,8-diboryl phenanthroline **8** (eq 2) under the conditions



(2)

of the borylation of THF catalyzed by Ir–**2b**, even at room temperature.<sup>30</sup> The initial rate of the borylation of THF conducted with Ir–**8** as a catalyst was identical to that observed when the reaction was conducted with the catalyst Ir–**2b** containing the unsubstituted phenanthroline. This equal reactivity and rapid borylation of the parent phenanthroline ligands implies that the active catalyst in the reactions conducted with **2b** contains the diborylated ligand **8**.

The Ir–CO complex **9** containing ligand **8** was prepared, and the C–O stretching frequency of this complex was 1973  $\text{cm}^{-1}$ . This value is close to that for the C–O stretching frequency of complex **5b** (1974  $\text{cm}^{-1}$ ) containing the parent phenanthroline ligand **2b**. While this result does not reconcile the lack of correlation depicted in Figure 3a, it does show that the substituents at the 3 and 8 positions of a phenanthroline can affect the rate of the corresponding reaction, even if they have little effect on the electron-donating ability of the ligand. This effect of the 3 and 8 substituent on the rate of the reaction will be described in detail later in this paper.

For the reactions catalyzed by complexes containing phenanthrolines **3a–e**, which contain the 3,8-dimethyl motif, a positive correlation between the log of  $k_{\text{obs}}$  and the electron density at Ir was observed (Figure 3b), with one exception: the reaction catalyzed by pyrrolidinyl-substituted Ir–**3e** was slower than that catalyzed by Ir–**3d** or Ir–**3c**, even though **3e** is more donating than **3c** or **3d**. Similarly, for the borylation of THF catalyzed by the 3,8-dimesityl-substituted series Ir–(**4a–d**), a positive correlation between the log of  $k_{\text{obs}}$  and the electron density at Ir was observed (Figure 3c). However, the rate of the borylation of THF catalyzed by Ir–**4d** containing silylmethyl groups at the 4 and 7 positions was slightly lower than the rate of the analogous reaction with Ir–**4c** as the catalyst with methyl groups at the 4 and 7 positions, even though **4d** is more donating than **4c**.

In general, the turnover frequencies (TOF) of reactions catalyzed by Ir catalysts containing phenanthrolines **4a–d** bearing the 3,8-dimesityl groups were higher than those of reactions catalyzed by analogous complexes containing phenanthrolines bearing either 3,8-dimethyl groups (**3a–e**) or no groups at the 3 and 8 positions (**2a–e**) (Table 2). However, the turnover number (TON) for reactions catalyzed by Ir–**3c** and Ir–**3d** (TON = 21 and 27, respectively) containing the 3,8-dimethyl motif were higher than those for reactions catalyzed by Ir–**4c** and Ir–**4d** (TON = 20 and 14, respectively) containing the 3,8-dimesityl groups. Thus, among the three series of phenanthrolines **2a–e**, **3a–e**, and **4a–d**, phenanthrolines containing the 3,8-dimesityl groups typically form the most active catalysts for the borylation of THF, and the phenanthrolines containing the 3,8-dimethyl motif typically generate catalysts that form the product from the borylation of THF in the highest yield.

### Investigation of the Trends in Catalyst Activity for the Borylation of THF Catalyzed by Ir–Phen Complexes.

To reveal the origins of the correlations of the relationships between  $\log(k_{\text{obs}})$  for the borylation of THF catalyzed by the phenanthroline-ligated iridium complexes and the electron density at the metal center of these catalysts, particularly the origin of the accelerating effect of the 3 and 8 substituents on the phenanthroline, we conducted experimental and computational studies.

The observation that phenanthrolines **4a–d** containing the 3,8-dimesityl motif form some of the most active catalysts for the borylation of THF suggested that a subtle effect unrelated to the electron density at the Ir center is influencing the rate. Because the electron-donating abilities of phenanthrolines containing either H, Me, or Mes at the 3 and 8 positions are similar to each other, the higher rates for the borylation of THF catalyzed by Ir–(**4a–d**) over those of reactions catalyzed by the analogous 3,8-unsubstituted or 3,8-methyl-substituted Ir–(**2a–d**) and Ir–(**3a–d**) cannot be rationalized by the relative electron densities at the Ir centers of these catalysts. Furthermore, the 3 and 8 substituents are too far from the metal center to affect the steric environment around Ir. However, the 3,8 substituents could affect the interligand interactions between the phenanthroline and the boryl groups of the Ir catalyst because the electron density at Ir might not reflect such effects.

In 2014, our group reported a method for the borylation of alkylamines catalyzed by the combination of ( $\eta^6$ -mes)Ir(Bpin)<sub>3</sub> and ligand **3c** that was selective for the borylation of



primary C–H bonds  $\beta$  to nitrogen over the borylation of primary C–H bonds  $\alpha$  to nitrogen.<sup>20</sup> A natural bond orbital (NBO)<sup>31</sup> analysis of the corresponding transition states for oxidative addition of the C–H bond calculated by DFT strongly suggested that the selectivity is derived from a set of weak interactions that are stronger in the transition state for the cleavage of a C–H bond  $\beta$  to nitrogen than in the transition state for the cleavage of a C–H bond  $\alpha$  to nitrogen. Of these interactions, C–H $\cdots$ O interactions between the C–H bonds at the 2,9 positions of the phenanthroline and the oxygen atoms of the boryl groups in the plane of the phenanthroline were the strongest. Because the 3 and 8 substituents on phenanthroline are ortho to the C–H bonds at the 2 and 9 positions, these substituents could affect this interligand C–H $\cdots$ O interaction, which could stabilize the transition state for oxidative addition, relative to the ground state.

To investigate the effect of the 3 and 8 substituents of phenanthrolines on the strength of the C–H $\cdots$ O interactions relevant to the borylation of alkyl C–H bonds catalyzed by Ir–phenanthroline complexes, we computed by DFT the ground states and transition states for the oxidative addition of THF by Ir–trisboryl complexes bound by ligands **2c**, **3c**, or **4c**. Each of these phenanthroline ligands contains the 4,7-dimethyl motif, but each has a different set of 3,8 substituents (H, Me, or Mes, respectively). The electron-donating ability of all three of the ligands is similar to each other. Computations of the ground states and transition states of the reactions of complexes containing ligands **2c**, **3c**, and **4c** revealed some structural differences between the binding of the three ligands. The phenanthrolines contained in Ir–**2c** and Ir–**3c** lay in the coordination plane (NN–Ir–B–B) while that in Ir–**4c** is tilted away from this plane by 20–27° (see the Supporting Information for Cartesian coordinates and structure images). A NBO analysis<sup>31</sup> of these structures allowed us to determine the energy of the C–H $\cdots$ O interactions ( $E_{\text{NBO}}$ ) in the ground states and transition states for the H–O contacts in which the H–O distance is less than the sum of the corresponding van der Waals radii (<2.72 Å) and the corresponding C–H–O angle is greater than 90°. For all three reactions, the energy of the C–H $\cdots$ O interactions between the C–H bonds at the 2,9 positions and the O atoms of the boryl ligands (see Figure 4a) in the transition state were greater than those in the ground state ( $E_{\text{NBO}}$  = negative). The H–O distances of these interactions ranged from 2.13 to 2.59 Å, and the corresponding C–H–O angles ranged from 123 to 145°. Furthermore, an additional C–H $\cdots$ O interaction was identified in the structures relevant to the reaction of THF and the Ir–trisboryl bound by **4c**. This interaction involves the benzylic C–H bond of the mesityl group contained in **4c** and the oxygen atoms of the boryl ligands (see Figure 4b). Although the H–O distances corresponding to this interaction were long (2.45 to 2.55 Å), the strength of the interaction energies was significant due to the corresponding angles (158 to 174°) being close to the ideal angle (180°) for C–H $\cdots$ O interactions. This interaction energy in the transition state was also computed to be larger than this interaction in the ground state ( $E_{\text{NBO}}$  = negative). Additional C–H $\cdots$ O interactions between THF and one of the boryl ligands were revealed in the NBO analysis for all three ligands. However, due to the similarities in structure for all three transition states, the sums of these interactions for all these structures were nearly identical to each other (1.53–1.63 kcal/mol, see Supporting Information pp. S38–S48 for details).

The total  $E_{\text{NBO}}$  for these reactions are provided in Table 3. In addition, Table 3 contains values for the computed barriers ( $G_{\text{comp}}^{\ddagger}$ ) of the reactions of THF with the phen-bound Ir-trisboryl complexes and the experimental barriers ( $G_{\text{exp}}^{\ddagger}$ ) of the corresponding catalytic reactions. The computed and experimentally determined barriers appear to correlate with

$E_{\text{NBO}}$ , suggesting that these C–H $\cdots$ O interactions may be the origin of the difference in rates for the borylation of THF catalyzed by the Ir catalysts containing ligands **2c**, **3c**, or **4c**. The NBO analysis of the structures involving ligand **4c** containing the 3,8-dimesityl motif shows that the stabilization of the transition state ( $E_{\text{NBO}} = -1.62$  kcal/mol) by C–H $\cdots$ O interactions in **4c** is greater than that of the structures corresponding to ligands **2c** ( $E_{\text{NBO}} = -1.14$  kcal/mol) and **3c** ( $E_{\text{NBO}} = -0.91$  kcal/mol). Thus, the trend in stabilization of the corresponding transition states containing each ligand follows the order **4c** > **3c** > **2c**, which matches the trend in reactivity of the corresponding catalysts determined computationally and experimentally. In general, the relative values of the computed barriers agree with those of the experimentally determined barriers. However, our calculations slightly overestimate the differences in reactivity of the corresponding catalysts.

The majority of the stabilization (0.92 kcal/mol out of 1.62 kcal/mol) of the transition state containing ligand **4c** by C–H $\cdots$ O interactions results from the interaction of benzylic C–H bonds of the mesityl groups with the O atoms of boryl ligands. Thus, these unique interactions make the Ir–**4c** catalyst more active than catalysts Ir–**2c** or Ir–**3c**. To test this hypothesis and the ability to capitalize on this C–H $\cdots$ O interaction, we designed two ligands in which the methyl groups on the 3,8-dimesityl motif are perturbed, and we sought to compare the activity of catalysts containing these ligands to the one containing 3,8-dimesitylphenanthroline **4b**. One ligand **10a** contains 2,4,6-trimethoxyphenyl groups at the 3 and 8 positions, and another ligand **10b** contains 2,4,6-tri-(methoxymethyl)phenyl groups at the 3 and 8 positions (Table 4). The corresponding CO complexes **11a** and **11b**, containing ligands **10a** and **10b**, respectively, were synthesized, and the C–O stretching frequencies were determined to be 1973 and 1974  $\text{cm}^{-1}$ , respectively. These values are similar to the C–O stretching frequency of complex **6b** (1974  $\text{cm}^{-1}$ ) containing 3,8-dimesitylphenanthroline **4b**.

If the benzylic C–H $\cdots$ O interaction contributes to the stabilization of transition states for the oxidative addition of THF containing phenanthrolines with the 3,8-dimesityl motif then one would expect that the activity of the catalyst containing ligand **10a** for the borylation of THF should be lower than that of the catalyst containing ligand **4b**, which is due to a lack of benzylic C–H bonds in ligand **10a**. In contrast, one would expect that the activity of the catalyst containing ligand **10b** should be higher than that of the catalyst containing ligand **4b** due to the enhanced acidity of the benzylic C–H bonds of ligand **10b** relative to those of ligand **4b**. This higher acidity should lead to stronger C–H $\cdots$ O interactions. Indeed, the borylation of THF catalyzed by Ir–**10a** showed that the activity of this catalyst (TOF = 0.16  $\text{h}^{-1}$ ) was much lower than that of Ir–**4b** (TOF = 1.3  $\text{h}^{-1}$ ). Furthermore, the activity of Ir–**10b** (TOF = 1.7  $\text{h}^{-1}$ ) for the borylation of THF was higher than that of Ir–**4b**. Thus, the activity for the borylation of THF of the catalysts containing ligands **4b**, **10a**, or **10b** span an order of magnitude, even though the electron-donating ability and steric properties of the corresponding three ligands are similar to each other.

## Discussion of the Importance of C–H···O Interactions on the Borylation of THF and Other Alkanes.

On the basis of our computational and experimental studies on the borylation of THF catalyzed by Ir–phen complexes, interligand interactions between the C–H bonds of the phenanthroline ligand and the O atoms of boryl ligands appear to be important stabilizing interactions in the transition state for the turnover-limiting C–H oxidative addition of THF. The strength of these interactions is independent of the ability of the ligand to donate electron density to Ir. Thus, these interactions may explain the lack of a strong correlation between the electron density at Ir and the log of the rate constant for the borylation of THF.

Because these C–H···O interactions are stronger in the transition state for oxidative addition of the C–H bond than in the ground state, the addition of THF to Ir–trisboryl to form the transition state for oxidative addition must perturb the coordination sphere of the transition state, relative to that of the ground state, in such a way that the boryl ligands are properly oriented to interact with C–H bonds of the phenanthroline. Such a perturbation could be explained by the steric penalty of adding a bulky secondary alkyl group to Ir in this transition state, forcing the coordination sphere to be more crowded. Thus, this steric penalty might be paid for, in part, by the attractive interactions between the boryl ligands and the phenanthroline. However, the corresponding transition state for oxidative addition of a substrate containing primary alkyl C–H bonds will be less crowded than that for the borylation of THF. As a result, changes in the C–H···O interactions during the borylation of primary alkyl C–H bonds could be less than those during the borylation of secondary alkyl C–H bonds.

To explore the effect of the size of the substrate (primary vs secondary alkyl) on the relative activity of catalysts for the borylation of alkanes, we extended our experimental and computational studies to the borylation of the primary alkyl C–H bonds in diethoxyethane. Like THF, diethoxyethane has C–H bonds  $\beta$  to oxygen that are particularly reactive toward borylation. We conducted the borylation of diethoxyethane catalyzed by Ir–**2c**, Ir–**3c**, or Ir–**4c** and measured the initial rates of formation of primary alkyl boronate ester **12** (Table 5). The turnover frequencies for the borylation of diethoxyethane catalyzed by Ir–**2c**, Ir–**3c**, or Ir–**4c** were nearly identical to each other (TOF = 17 h<sup>-1</sup>, 16 h<sup>-1</sup>, and 20 h<sup>-1</sup>, respectively). In contrast, the turnover frequencies for the borylation of THF catalyzed by the same set of catalysts varied measurably (TOF = 0.82 h<sup>-1</sup>, 0.86 h<sup>-1</sup>, and 2.3 h<sup>-1</sup>, respectively). Thus, C–H···O interactions could be a less important set of stabilizing interactions in the transition state for the borylation of substrates containing primary C–H bonds than for the borylation of substrates containing secondary C–H bonds.

To compare the changes in C–H···O interactions during the borylation of diethoxyethane to those during the borylation of THF, we computed the oxidative addition of the C–H bond of a truncated, but representative, substrate ethyl methyl ether to the Ir–trisboryl complex bound by ligand **3c**. We compared the C–H···O distances in the ground state (Figure 5a, **GS**) and the transition state for the oxidative addition of THF (Figure 5b, **TS-I**) to those of the analogous transition state and ground state for the oxidative addition of diethoxyethane (Figure 5c, **TS-II**). In the ground state **GS**, the distance between H2 and O2 (2.133 Å) is the

only H $\cdots$ O distance that is less than the sum of the van der Waals radii, and the corresponding C–H $\cdots$ O interaction energy is quite large ( $E_{\text{NBO}} = 4.87$  kcal/mol). In the transition state for oxidative addition of THF, the H2–O2 distance is only slightly longer (changing from 2.133 to 2.149 Å), but the H1–O1 distance is dramatically shorter (changing from 2.977 to 2.344 Å), forming a second C–H $\cdots$ O interaction and leading to an overall stabilization of the transition state ( $E_{\text{NBO}} = -1.14$  kcal/mol). In contrast, in the transition state for the oxidative addition of ethyl methyl ether, the H2–O2 is significantly longer (changing from 2.133 to 2.279 Å) and the H1–O1 distance is shorter (changing from 2.977 to 2.341 Å) and is similar to that observed for the oxidative addition of THF. Overall, for the oxidative addition of ethyl methyl ether, the C–H $\cdots$ O interaction energies are larger in the ground state than in the transition state ( $E_{\text{NBO}} = +0.69$  kcal/mol) due to the significantly longer H2–O2 distance in the transition state than in the ground state.

Thus, our calculations predict that the C–H $\cdots$ O interactions between the phenanthroline and the boryl ligands do not stabilize the transition state for oxidative addition of the C–H bond of diethoxyethane, relative to the ground state. In this case, catalysts that have similar electron-densities at Ir to one another should catalyze the borylation of diethoxyethane at similar rates. This prediction is consistent with our experimental results (see Table 5). Both our calculations and our experimental results suggest that the effect of the C–H $\cdots$ O interactions between the phenanthroline and the boryl ligands on the borylation of secondary alkyl C–H bonds is larger than it is on the rate of borylation of primary alkyl C–H bonds. This difference is likely due to the greater crowding of the transition state for oxidative addition of a secondary alkyl C–H bond relative to that of the transition state for the oxidative addition of a primary alkyl C–H bond, and this greater crowding leads to stronger interligand interactions between the phenanthroline and the boryl ligands.

During the course of this work, Sakaki published a computational study about the origins of the selectivity for functionalization of the C–H bond  $\beta$  to oxygen in THF over the C–H bond  $\alpha$  to oxygen.<sup>32</sup> This study suggested that the selectivity results from reversible oxidative addition of the C–H bond  $\alpha$  to oxygen due to a high barrier for reductive elimination from the resulting alkyl complex with the  $\alpha$  carbon bound to iridium. These calculations also suggested that the oxidative addition of the C–H bond  $\beta$  to oxygen is reversible, but the primary, albeit relatively small, kinetic isotope effect of 2.6 we have measured for the borylation of THF clearly shows that the energy of the transition state for oxidative addition of the C–H bond  $\beta$  to oxygen is higher or nearly equal to that of the transition state for reductive elimination. Thus, the studies we report here show how the electronic properties of the ancillary ligand and nonbonded attractive secondary interactions involving substituents on the ligand influence the rates of the oxidative addition step of the catalytic cycle, rather than steps occurring after the oxidative addition.

Also during the course of this investigation, Sawamura and co-workers reported an enantioselective, directed borylation of alkyl C–H bonds.<sup>33</sup> Computational studies implied that a series of noncovalent interactions, including C–H $\cdots$ O interactions, contributed to the observed selectivity. These findings corroborate our proposal that the sum of these weak interactions can lead to significant differences in reactivity.

## CONCLUSIONS

In summary, we have conducted a detailed study of the effect of the electronic properties of phenanthroline ligands on the electron-donating ability of these ligands and on the rates for cleavage of C–H bonds by iridium–trisboryl complexes that catalyze the borylation of C–H bonds. Our data reveal several factors that control the rates of the catalytic reaction and that could direct the design of future catalysts:

1. Variations of the 4,7 substituent of phenanthrolines can significantly alter the electron-donating property of phenanthrolines. In general, for phenanthrolines containing the same 3 and 8 substituents, the rates of the borylation of THF catalyzed by more electron-rich Ir catalysts are faster than those catalyzed by more electron-poor Ir catalysts.
2. The effect of varying the 3 and 8 substituents from H to Me or Mes on the electron-donating ability of the ligand is small, but these substituents can have a large effect on the rate of the borylation of THF catalyzed by the corresponding Ir–phen complex. Among ligands **2–4**, phenanthrolines containing the 3,8-dimesityl motif form the most active catalysts for the borylation of THF.
3. Computational and experimental studies suggest that C–H $\cdots$ O interactions between the phenanthroline and boryl ligands stabilize the transition state for oxidative addition of the secondary C–H bonds of THF to Ir–trisboryl complexes relative to the ground state. In contrast, these interactions do not stabilize the transition state for the oxidative addition of the primary C–H bonds of EtOMe relative to the ground state.

Our computational and experimental results suggest that the structure of phenanthrolines can be modified to increase the strength of these C–H $\cdots$ O interactions, which may affect the rates of the borylation of secondary alkyl C–H bonds catalyzed by Ir–phen complexes differently from the way they affect the rates of the borylation of primary alkyl C–H bonds. Although synthetic chemists typically consider the electronic and steric properties of the metal center when designing new catalysts, the present study underscores how weak interactions within the coordination sphere should be considered as part of catalyst design.

## Supplementary Material

Refer to Web version on PubMed Central for supplementary material.

## ACKNOWLEDGMENTS

We also thank Dr. A. DiPasquale for X-ray crystallography assistance.

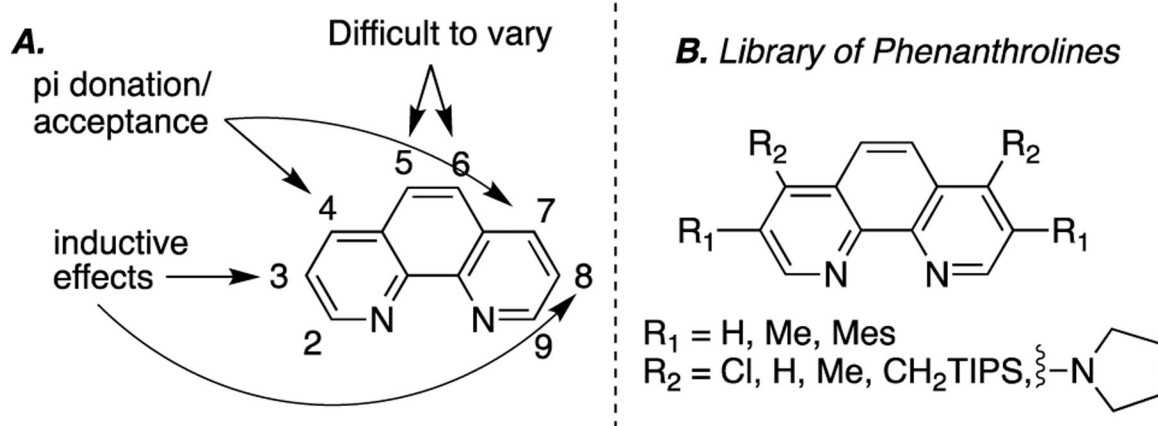
### Funding

We thank the NIH for support of J.F.H. (R35GM130387), for support of the Molecular Graphics and Computation Facility at UC Berkeley (S10OD023532), for support of the CoC NMR facility (S10OD024998), and for support of the X-ray facility (S10-RR027172). M.A.L. thanks Chevron and the ACS DOC for predoctoral fellowships. R.J.O. thanks the Swiss National Science Foundation for a Postdoctoral Fellowship. We thank Johnson Matthey for a gracious donation of [Ir(COD)OMe]<sub>2</sub>.

## REFERENCES

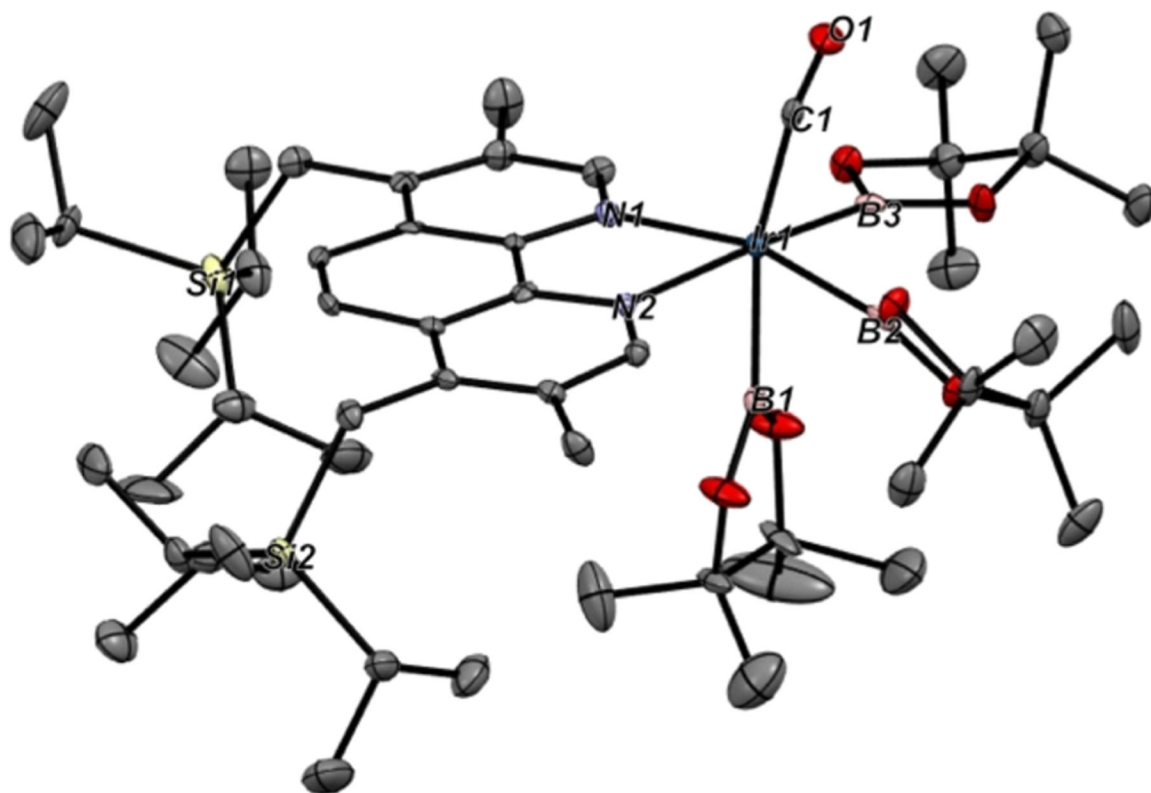
- (1). Goldberg KI; Goldman AS Activation and Functionalization of C-H Bonds; 2004.
- (2). Godula K; Sames D C-H Bond Functionalization in Complex Organic Synthesis. *Science* 2006, 312, 67. [PubMed: 16601184]
- (3). Hartwig JF Evolution of C-H Bond Functionalization from Methane to Methodology. *J. Am. Chem. Soc* 2016, 138, 2. [PubMed: 26566092]
- (4). Hartwig JF; Larsen MA Undirected, Homogeneous C-H Bond Functionalization: Challenges and Opportunities. *ACS Cent. Sci* 2016, 2, 281. [PubMed: 27294201]
- (5). Mkhaliid IAI; Barnard JH; Marder TB; Murphy JM; Hartwig JF C-H Activation for the Construction of C-B Bonds. *Chem. Rev* 2010, 110, 890. [PubMed: 20028025]
- (6). Campeau L-C; Chen Q; Gauvreau D; Girardin M; Belyk K; Maligres P; Zhou G; Gu C; Zhang W; Tan L; O'Shea PD A Robust Kilo-Scale Synthesis of Doravirine. *Org. Process Res. Dev* 2016, 20, 1476.
- (7). Ishiyama T; Takagi J; Ishida K; Miyaura N; Anastasi NR; Hartwig JF Mild Iridium-Catalyzed Borylation of Arenes. High Turnover Numbers, Room Temperature Reactions, and Isolation of a Potential Intermediate. *J. Am. Chem. Soc* 2002, 124, 390. [PubMed: 11792205]
- (8). Ishiyama T; Takagi J; Hartwig JF; Miyaura N A Stoichiometric Aromatic C-H Borylation Catalyzed by Iridium(I)/2,2'-Bipyridine Complexes at Room Temperature. *Angew. Chem., Int. Ed* 2002, 41, 3056.
- (9). Chen H; Schlecht S; Semple TC; Hartwig JF Thermal, Catalytic, Regiospecific Functionalization of Alkanes. *Science* 2000, 287, 1995. [PubMed: 10720320]
- (10). Murphy JM; Lawrence JD; Kawamura K; Incarvito C; Hartwig JF Ruthenium-Catalyzed Regiospecific Borylation of Methyl C-H Bonds. *J. Am. Chem. Soc* 2006, 128, 13684. [PubMed: 17044685]
- (11). Liskey CW; Hartwig JF Iridium-Catalyzed Borylation of Secondary C-H Bonds in Cyclic Ethers. *J. Am. Chem. Soc* 2012, 134, 12422. [PubMed: 22804581]
- (12). Ohmura T; Torigoe T; Sugimoto M Iridium-catalysed borylation of sterically hindered C(sp<sup>3</sup>)-H bonds: remarkable rate acceleration by a catalytic amount of potassium tert-butoxide. *Chem. Commun* 2014, 50, 6333.
- (13). Lawrence JD; Takahashi M; Bae C; Hartwig JF Regiospecific Functionalization of Methyl C-H Bonds of Alkyl Groups in Reagents with Heteroatom Functionality. *J. Am. Chem. Soc* 2004, 126, 15334. [PubMed: 15563132]
- (14). Liskey CW; Hartwig JF Iridium-Catalyzed C-H Borylation of Cyclopropanes. *J. Am. Chem. Soc* 2013, 135, 3375. [PubMed: 23421575]
- (15). Kawamorita S; Miyazaki T; Iwai T; Ohmiya H; Sawamura M Rh-Catalyzed Borylation of N-Adjacent C(sp<sup>3</sup>)-H Bonds with a Silica-Supported Triarylphosphine Ligand. *J. Am. Chem. Soc* 2012, 134, 12924. [PubMed: 22816772]
- (16). Kawamorita S; Murakami R; Iwai T; Sawamura M Synthesis of Primary and Secondary Alkylboronates through Site-Selective C(sp<sup>3</sup>)-H Activation with Silica-Supported Monophosphine-Ir Catalysts. *J. Am. Chem. Soc* 2013, 135, 2947. [PubMed: 23398347]
- (17). Zhang L-S; Chen G; Wang X; Guo Q-Y; Zhang X-S; Pan F; Chen K; Shi Z-J Direct Borylation of Primary C-H Bonds in Functionalized Molecules by Palladium Catalysis. *Angew. Chem., Int. Ed* 2014, 53, 3899.
- (18). Larsen MA; Cho SH; Hartwig J Iridium-Catalyzed, Hydrosilyl-Directed Borylation of Unactivated Alkyl C-H Bonds. *J. Am. Chem. Soc* 2016, 138, 762. [PubMed: 26745739]
- (19). He J; Jiang H; Takise R; Zhu R-Y; Chen G; Dai H-X; Dhar TGM; Shi J; Zhang H; Cheng PTW; Yu J-Q Ligand-Promoted Borylation of C(sp<sup>3</sup>)-H Bonds with Palladium(II) Catalysts. *Angew. Chem., Int. Ed* 2016, 55, 785.
- (20). Li Q; Liskey CW; Hartwig JF Regioselective Borylation of the C-H Bonds in Alkylamines and Alkyl Ethers. Observation and Origin of High Reactivity of Primary C-H Bonds Beta to Nitrogen and Oxygen. *J. Am. Chem. Soc* 2014, 136, 8755. [PubMed: 24836159]

- (21). Preshlock SM; Ghaffari B; Maligres PE; Krska SW; Maleczka RE; Smith MR High-Throughput Optimization of Ir-Catalyzed C–H Borylation: A Tutorial for Practical Applications. *J. Am. Chem. Soc* 2013, 135, 7572. [PubMed: 23534698]
- (22). Larsen MA; Hartwig JF Iridium-Catalyzed C–H Borylation of Heteroarenes: Scope, Regioselectivity, Application to Late-Stage Functionalization, and Mechanism. *J. Am. Chem. Soc* 2014, 136, 4287. [PubMed: 24506058]
- (23). Ohmura T; Torigoe T; Suginome M Catalytic Functionalization of Methyl Group on Silicon: Iridium-Catalyzed C(sp<sup>3</sup>)–H Borylation of Methylchlorosilanes. *J. Am. Chem. Soc* 2012, 134, 17416. [PubMed: 23043232]
- (24). Altman RA; Buchwald SL 4,7-Dimethoxy-1,10-phenanthroline: An Excellent Ligand for the Cu-Catalyzed N-Arylation of Imidazoles. *Org. Lett* 2006, 8, 2779. [PubMed: 16774255]
- (25). Schmittel M; Ammon H A Short Synthetic Route to 4,7-Dihalogenated 1,10-Phenanthrolines with Additional Groups in 3,8-Position: Soluble Precursors for Macrocyclic Oligophenanthrolines. *Eur. J. Org. Chem* 1998, 1998, 785.
- (26). Thiele S; Malmgaard-Clausen M; Engel-Andreasen J; Steen A; Rummel PC; Nielsen MC; Gloriam DE; Frimurer TM; Ulven T; Rosenkilde MM Modulation in Selectivity and Allosteric Properties of Small-Molecule Ligands for CC-Chemokine Receptors. *J. Med. Chem* 2012, 55, 8164. [PubMed: 22957890]
- (27). Larsen MA; Wilson CV; Hartwig JF Iridium-Catalyzed Borylation of Primary Benzylic C–H Bonds without a Directing Group: Scope, Mechanism, and Origins of Selectivity. *J. Am. Chem. Soc* 2015, 137, 8633. [PubMed: 26076367]
- (28). Hansch C; Leo A; Taft RW A survey of Hammett substituent constants and resonance and field parameters. *Chem. Rev* 1991, 91, 165.
- (29). Chotana GA; Vanchura IIBA; Tse MK; Staples RJ; Maleczka JRE; Smith IIMR Getting the sterics just right: a five-coordinate iridium trisboryl complex that reacts with C–H bonds at room temperature. *Chem. Commun* 2009, 5731.
- (30). For the borylation of 4,4'-ditert-butyl bipyridine complexes and a complex of 3,4,7,8-tetramethylphenanthroline during catalytic borylation see: Oeschger RJ; Larsen MA; Bismuto A; Hartwig JF. Origin of the Difference in Reactivity between Ir Catalysts for the Borylation of C–H Bonds. *J. Am. Chem. Soc* 2019, 141, 16479. [PubMed: 31539230]
- (31). Glendening ED; Reed AE; Carpenter JE; Weinhold F NBO, version 3.1; University of Wisconsin: Madison, WI, 1996.
- (32). Zhong R-L; Sakaki S sp<sup>3</sup> C–H Borylation Catalyzed by Iridium(III) Triboryl Complex: Comprehensive Theoretical Study of Reactivity, Regioselectivity, and Prediction of Excellent Ligand. *J. Am. Chem. Soc* 2019, 141, 9854. [PubMed: 31124356]
- (33). Reyes RL; Iwai T; Maeda S; Sawamura M Iridium-Catalyzed Asymmetric Borylation of Unactivated Methylene C(sp<sup>3</sup>)–H Bonds. *J. Am. Chem. Soc* 2019, 141, 6817. [PubMed: 30983334]

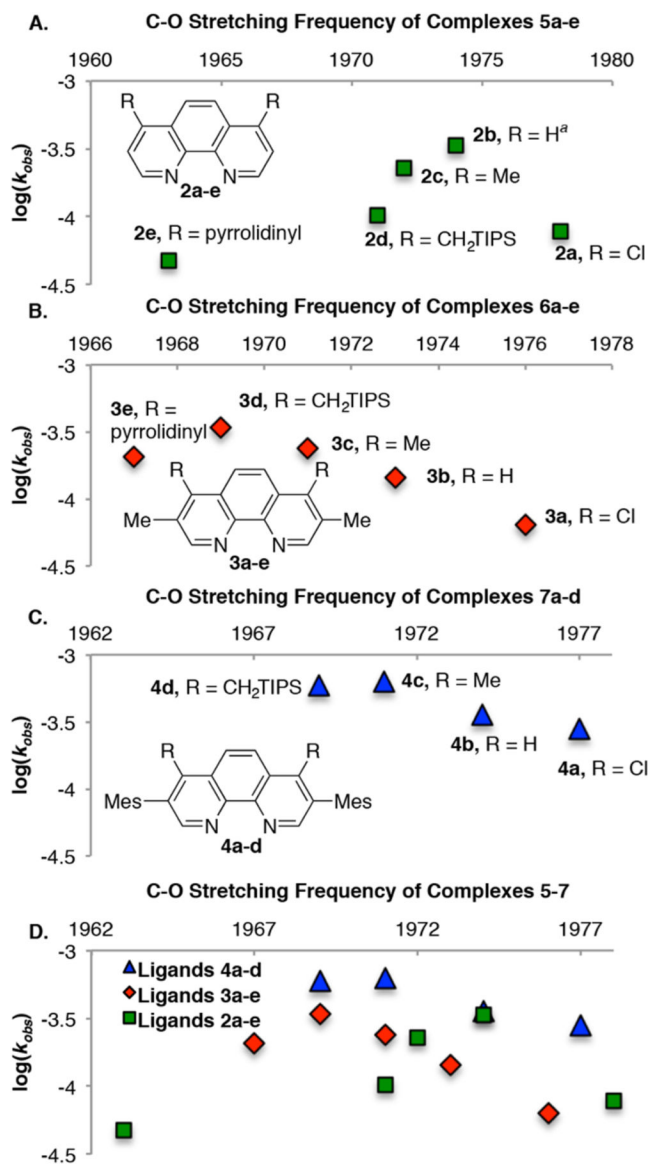


**Figure 1.**  
 (A) Properties and synthetic variability of the different positions for substitution on the phenanthroline core. (B) Overall design of a library of phenanthrolines.

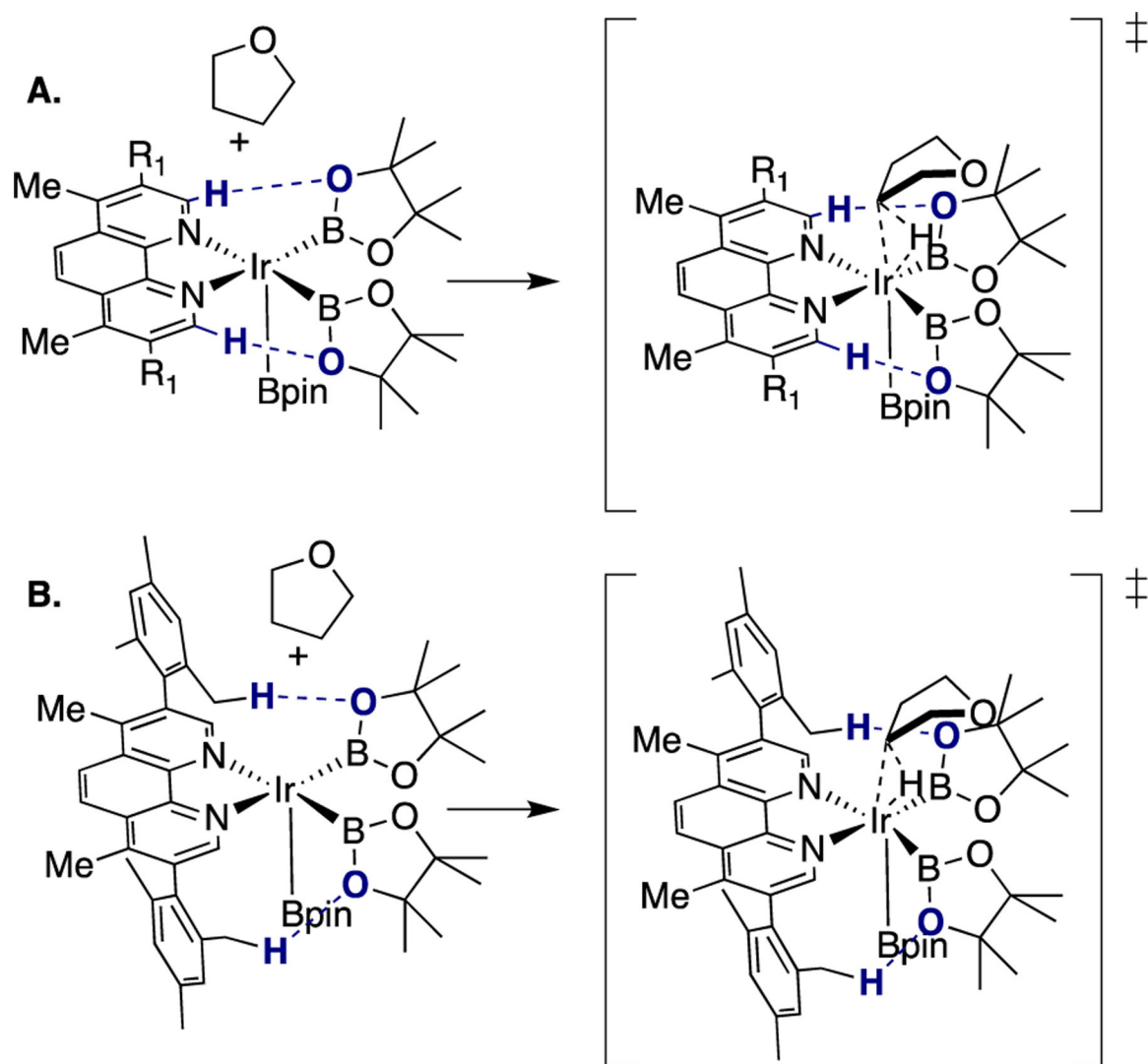




**Figure 2.** Structure of complex **6d** determined by single crystal X-ray diffraction. Hydrogen atoms have been omitted for clarity.

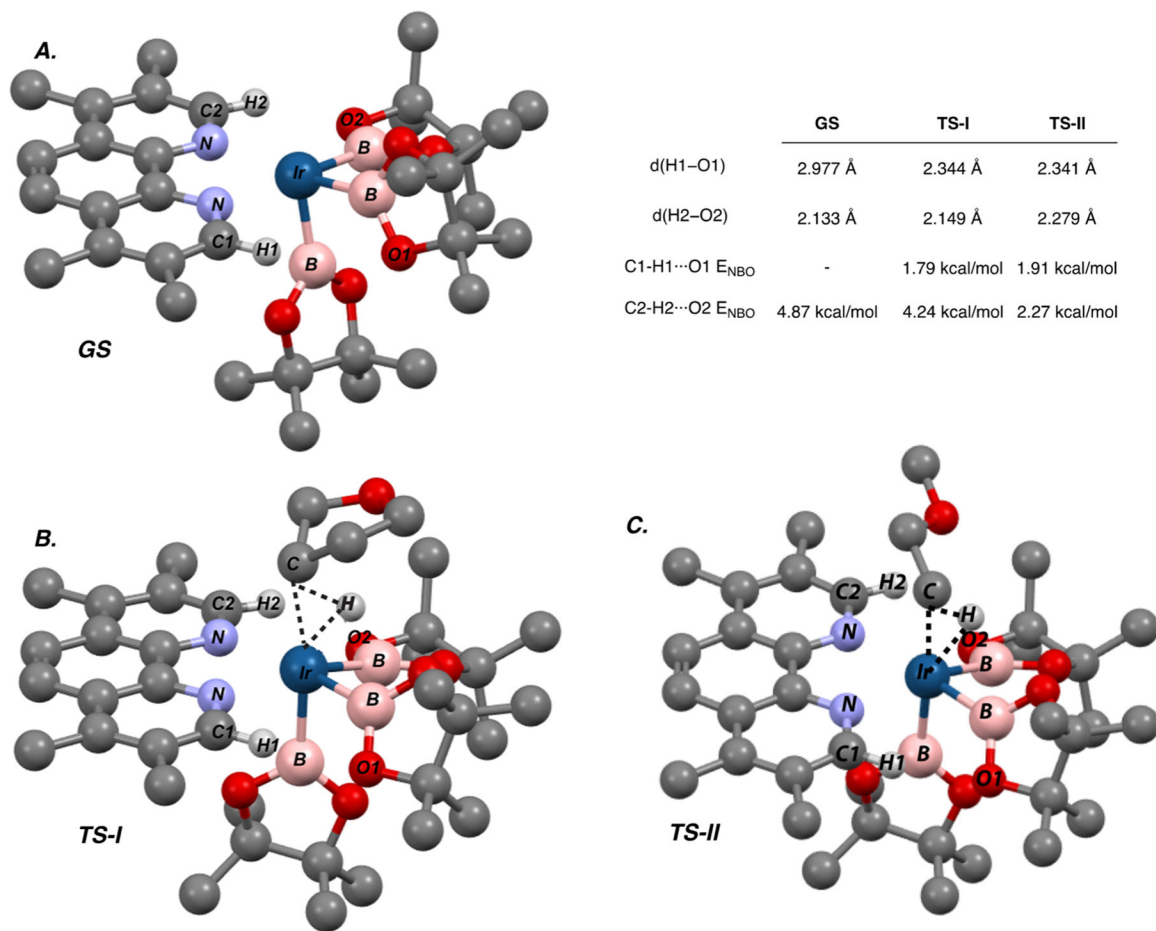


**Figure 3.** Effect of electron-donating ability (measured as a C–O stretching frequency) of phenanthroline ligands on the rates of the following reactions: (A) borylation of THF with B<sub>2</sub>pin<sub>2</sub> catalyzed by Ir–(2a–e), (B) borylation of THF with B<sub>2</sub>pin<sub>2</sub> catalyzed by Ir–(3a–e), and (C) borylation of THF with B<sub>2</sub>pin<sub>2</sub> catalyzed by Ir–(4a–d). (D) Superimposition of Figure 3a–c. <sup>a</sup>Phenanthroline 2b undergoes borylation to form ligand 8. See below.



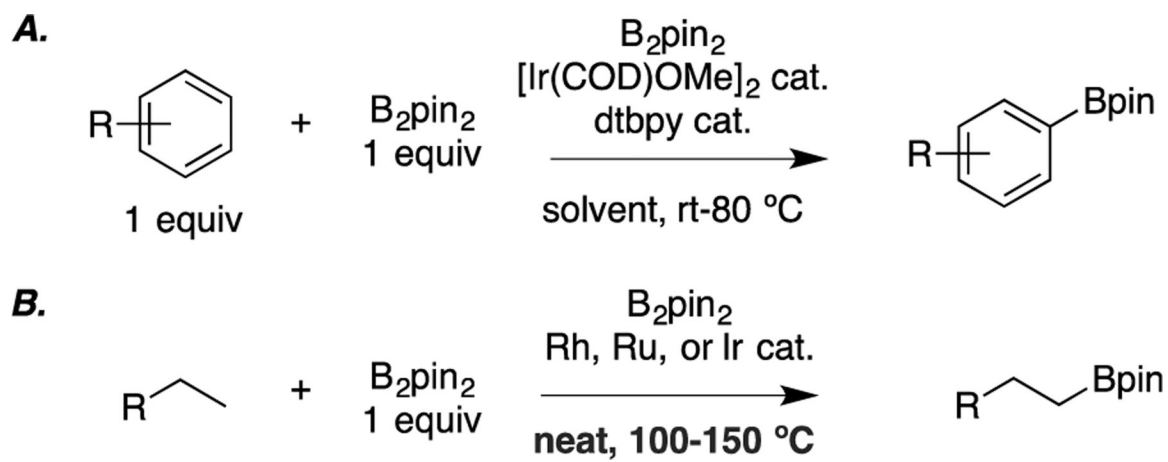
**Figure 4.**

(A) Interactions between the C-H bonds at the 2,9 positions of phenanthrolines and the oxygen atoms of boryl ligands in the ground state, and oxidative addition transition states for the reaction of THF with phen-bound Ir-trisboryl complexes. (B) Interaction of the benzylic C-H bonds of a mesityl group and the oxygen atoms of boryl ligands.

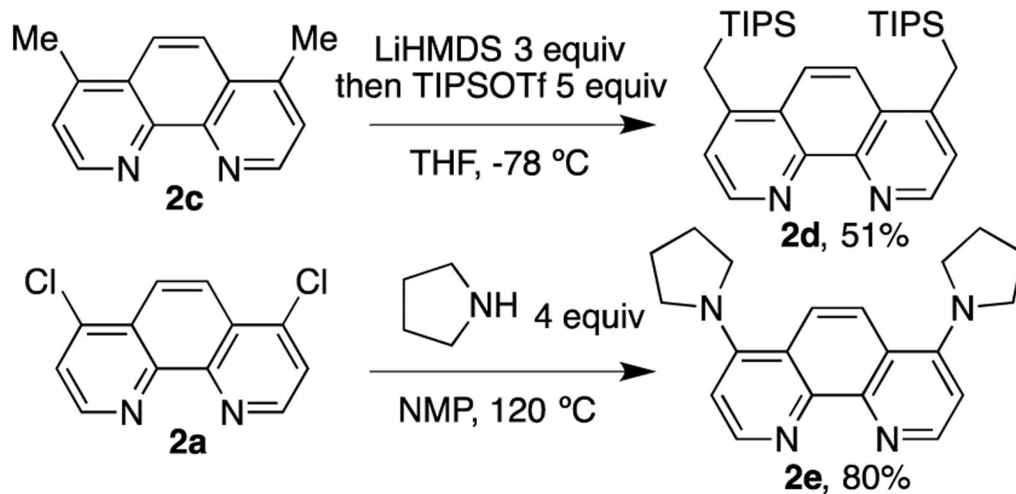
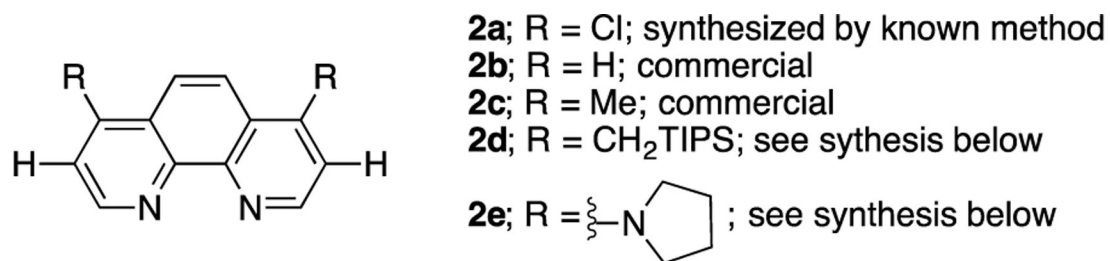


**Figure 5.**

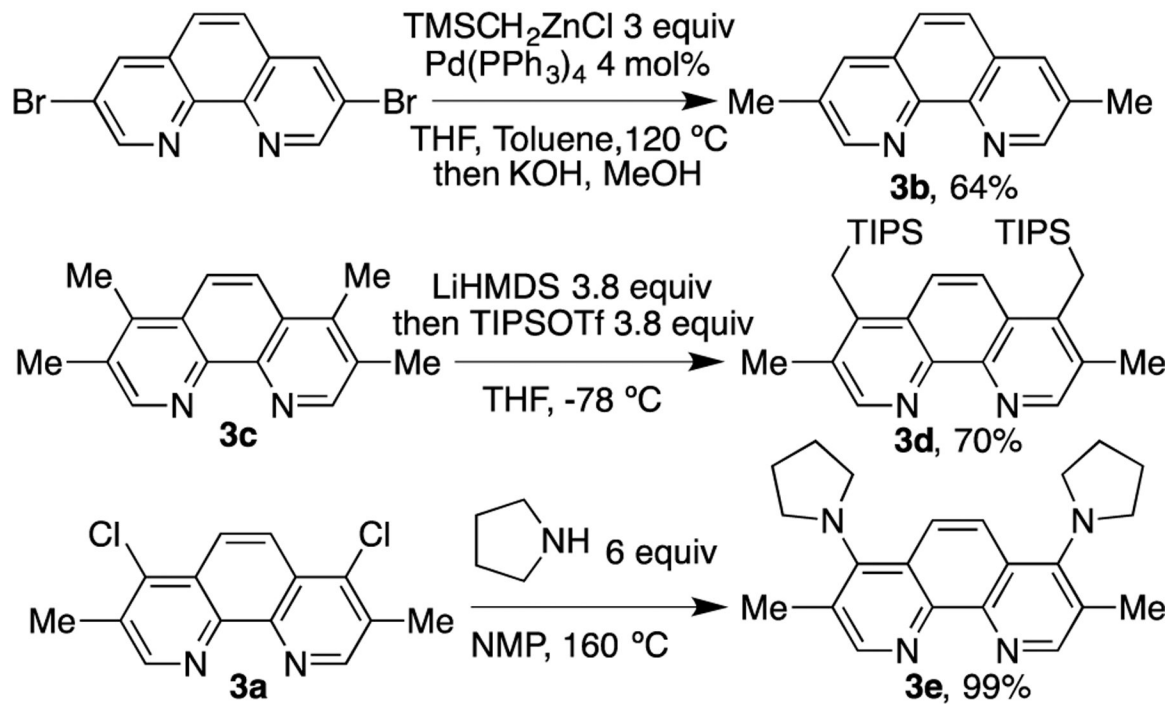
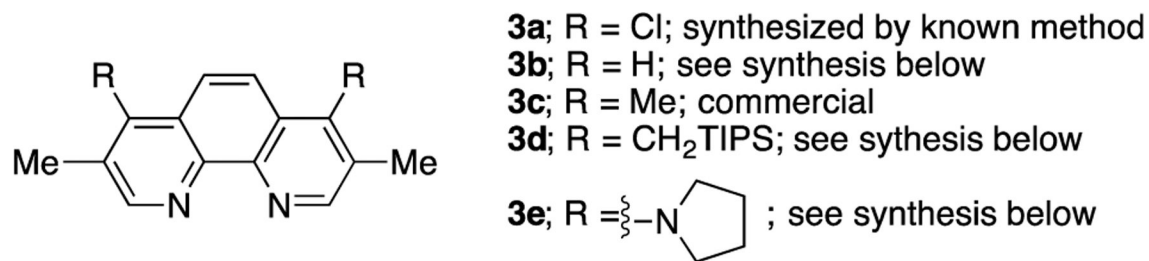
Frequency calculations (at  $T = 373$  K), optimization, and NBO analysis of ground states and transition states were conducted with the 6–31g(d,p)/lanl2dz basis set and the B3LYP-D3 functional. Single-point energy calculations were conducted with the 6–311++g\*\*/lanl2tz basis set and the M06 functional. (A) Ground state of Ir–trisboryl bound by **3c**. (B) Oxidative addition of THF to the Ir–trisboryl bound by **3c**. (C) Oxidative addition of EtOMe to the Ir–trisboryl bound by **3c**.

**Scheme 1.**

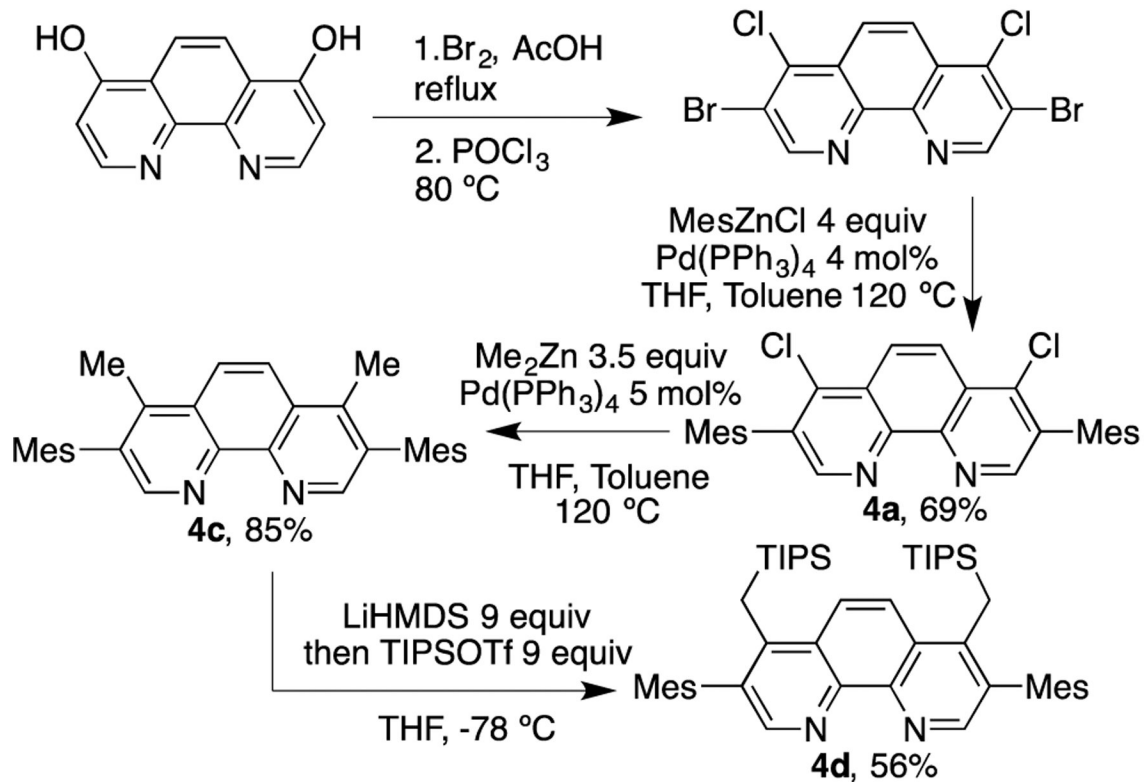
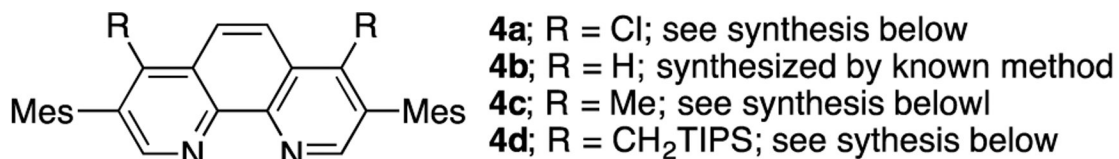
Comparison of Aryl C-H Borylation to Alkyl C-H Borylation



**Scheme 2.**  
Synthesis of 4,7-Disubstituted Phenanthrolines



**Scheme 3.**  
Synthesis of 3,8-Dimethylphenanthrolines



**Scheme 4.**  
Synthesis of 3,8-Dimesitylphenanthrolines



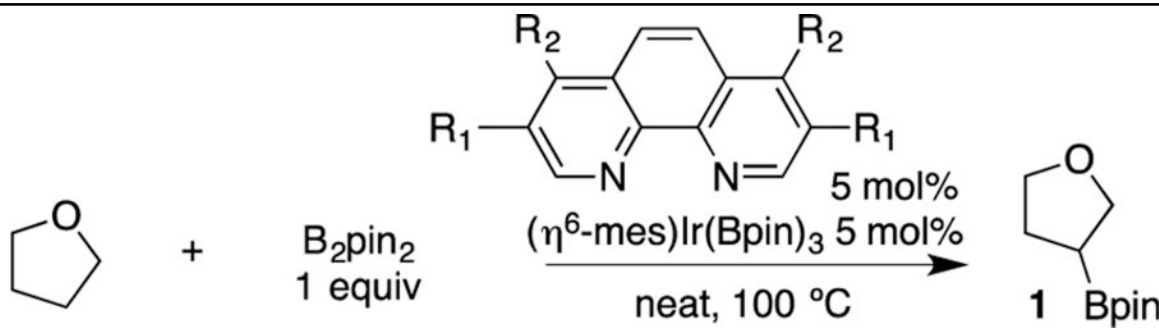
**Table 1.**

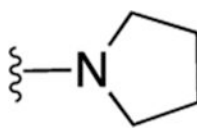
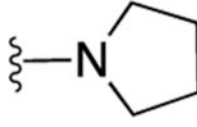
C–O Stretching Frequencies for a Series of Phenanthroline-Bound Ir–Trisboryl Carbon Monoxide Complexes

Reaction scheme: Phenanthroline derivative (2-4) +  $\frac{1}{2} [\text{Ir}(\text{COD})\text{OMe}]_2 \xrightarrow[\text{Cy-H, THF}]{\text{COE xs, HBpin xs then CO 1 atm}}$  Ir-trisboryl CO complex (5-7)

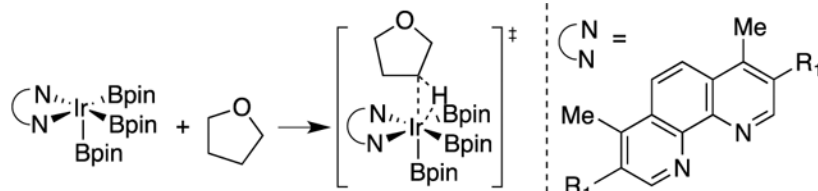
C–O stretch (complex)	R <sub>2</sub> = Cl	H	Me	ch <sub>2</sub> Tips	
R <sub>1</sub> = H	1978 cm <sup>-1</sup> ( <b>5a</b> )	1974 cm <sup>-1</sup> ( <b>5b</b> )	1972 cm <sup>-1</sup> ( <b>5c</b> )	1971 cm <sup>-1</sup> ( <b>5d</b> )	1963 cm <sup>-1</sup> ( <b>5e</b> )
Me	1976 cm <sup>-1</sup> ( <b>6a</b> )	1973 cm <sup>-1</sup> ( <b>6b</b> )	1971 cm <sup>-1</sup> ( <b>6c</b> )	1969 cm <sup>-1</sup> ( <b>6d</b> )	1967 cm <sup>-1</sup> ( <b>6e</b> )
Mes	1977 cm <sup>-1</sup> ( <b>7a</b> )	1974 cm <sup>-1</sup> ( <b>7b</b> )	1971 cm <sup>-1</sup> ( <b>7c</b> )	1969 cm <sup>-1</sup> ( <b>7d</b> )	-

Table 2.

C–H Borylation of THF Catalyzed By Various Ir–Phenanthroline Catalysts<sup>a</sup>


Ligand	R <sub>1</sub>	R <sub>2</sub>	Yield <sup>b</sup>	TON	TOF (h <sup>-1</sup> )
2a	H	Cl	15%	3.0	0.28
2b (8)	H (Bpin)	H	42% (50%)	8.0 (9.5)	1.7 (1.5)
2c	H	Me	23%	4.5	0.82
2d	H	CH <sub>2</sub> TIPS	55%	11	0.38
2e	H		33%	6.6	0.53
3a	Me	Cl	23%	4.6	0.23
3b	Me	H	100%	20	0.63
3c	Me	Me	103%	21	0.86
3d	Me	CH <sub>2</sub> TIPS	137%	27	1.2
3e	Me		89%	18	0.74
4a	Mes	Cl	28%	5.6	1.0
4b	Mes	H	97%	20	1.3
4c	Mes	Me	99%	20	2.3
4d	Mes	CH <sub>2</sub> TIPS	70%	14	2.1

<sup>a</sup>Reactions conducted on a 0.170 mmol scale.<sup>b</sup>Yields were determined by gas chromatography and are based on moles of B<sub>2</sub>pin<sub>2</sub>.

**Table 3.**Comparisons of C–H···O Interactions Calculated by DFT<sup>a</sup>


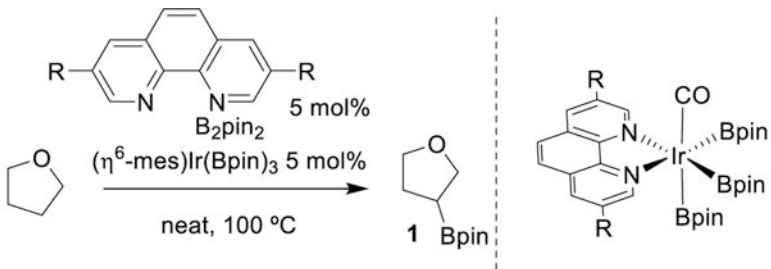
Ligand	R	C–H···O interactions		
		$\Delta E_{\text{NBO}}$ (relative)	$\Delta G_{\text{comp}}^{\ddagger b}$ (relative)	$\Delta G_{\text{exp}}^{\ddagger c}$ (relative)
<b>2c</b>	H	-0.91 (0.0)	33.4 (0.0)	30.0 (0.0)
<b>3c</b>	Me	-1.14 (-0.23)	32.4 (-1.0)	29.9 (-0.1)
<b>4c</b>	Mes	-1.62 (-0.71)	30.7 (-2.3)	29.2 (-0.8)

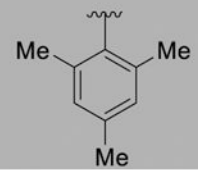
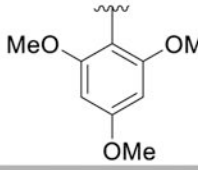
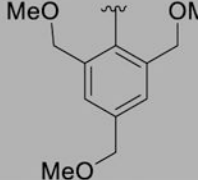
<sup>a</sup>Frequency calculations (at  $T = 373$  K), optimization, and NBO analysis of ground states and transition states were conducted with the 6-31g(d,p)/lanl2dz basis set and the B3LYP-D3 functional. Single-point energy calculations were conducted with the 6-311++g\*\*/lanl2tz basis set and the M06 functional.

<sup>b</sup>Computed barrier to oxidative addition of THF to phen-bound Ir–trisboryl complexes.

<sup>c</sup>Experimentally determined barrier for the borylation of THF catalyzed by Ir–phen complexes.

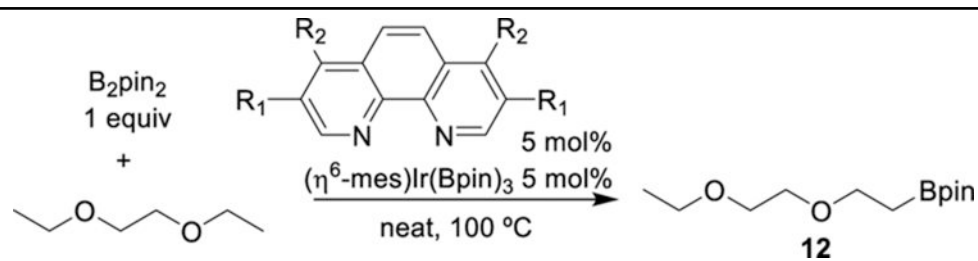
Table 4.

Borylation of THF Catalyzed by Ir Complexes Containing Phenanthrolines with 3,8-Diaryl Motifs<sup>a</sup>


Ligand	R	TOF (h <sup>-1</sup> )	complex	C-O stretching frequency
<b>4b</b>		1.3	<b>6b</b>	1974 cm <sup>-1</sup>
<b>10a</b>		0.16	<b>11a</b>	1973 cm <sup>-1</sup>
<b>10b</b>		1.7	<b>11b</b>	1974 cm <sup>-1</sup>

<sup>a</sup>Reactions conducted on a 0.170 mmol scale.

Table 5.

C–H Borylation of Diethoxyethane Catalyzed By Various Ir–Phenanthroline Catalysts<sup>a</sup>

ligand	R <sub>1</sub>	R <sub>2</sub>	TOF (h <sup>-1</sup> )	TON
2c	H	Me	17	27
3c	Me	Me	16	33
4c	Me	Mes	20	34

<sup>a</sup>Reactions conducted on a 0.170 mmol scale.